

Now the equations can be formally solved as

$$Z_0 = [S_{01}(E_{11} + S_{11} - C_{11})^{-1}S_{10} + i\varepsilon]^{-1}S_{01}(E_{11} + S_{11} - C_{11})^{-1}W_1, \quad (5.6)$$

$$Z_1 = (E_{11} + S_{11} - C_{11})^{-1}[1 - S_{10}\{S_{01}(E_{11} + S_{11} - C_{11})^{-1}S_{10} + i\varepsilon\}^{-1}S_{01}(E_{11} + S_{11} - C_{11})^{-1}]W_1. \quad (5.7)$$

In this form, we can study the limiting behavior of the solutions for small k and ε .

In the rapid limit where we first let $k \rightarrow 0$ and then $\varepsilon \rightarrow 0$,

$$\begin{aligned} Z_0 &= 0, \\ Z_1 &= -C_{11}^{-1}W_1. \end{aligned} \quad (5.8)$$

From Eq. (3.11) we have

$$\begin{aligned} \lim_{\varepsilon \rightarrow 0} \lim_{k \rightarrow 0} G_{j_a j_\gamma}(\mathbf{k}, \varepsilon + i\eta) / i\varepsilon \\ = \beta \sum_Q v_\gamma(Q) n_Q (n_Q + 1) \omega_Q Y_Q^{(-)}(\alpha), \end{aligned} \quad (5.9)$$

where $Y_Q^{(-)}(\alpha)$ satisfies the equation

$$\sum_{Q'} P_{QQ'} Y_{Q'}^{(-)}(\alpha) = -v_\alpha(Q) \omega_Q n_Q (n_Q + 1). \quad (5.10)$$

Equation (5.9) is just the expression for the static thermal conductivity given by the linearized Peirels-Boltzmann equation (5.10).

In the slow limit, $\varepsilon \rightarrow 0$ first and then $k \rightarrow 0$. So we expand Eqs. (5.6) and (5.7) in powers of ε , and with the help of the identity for the column vector

$$\sum_\gamma W_1(\mathbf{k}\gamma, \varepsilon) i k_\gamma = (\mu\beta)^{-1} S_{10}, \quad (5.11)$$

we obtain, for small ε ,

$$\begin{aligned} G_{hh}(\mathbf{k}, \varepsilon + i\eta) \\ = C_\gamma T [1 - i\varepsilon \{S_{01}(S_{11} - C_{11})^{-1}S_{10}\}^{-1}]. \end{aligned} \quad (5.12)$$

From this, we obtain the limit (2.15), within the error of terms of order r and, from Eq. (2.22), we see that $\kappa_{\alpha\gamma}(\mathbf{k}, \varepsilon + i\eta)$ tends to the static value given by (5.9) in the slow limit as well as in the rapid limit.

ACKNOWLEDGMENTS

I am grateful to Professor A. A. Maradudin for a critical reading of the manuscript and to Dr. A. Griffin for stimulating discussions.

Internal-Friction and Young's-Modulus Variations in the Superconducting, Mixed, and Normal States of Niobium*

EDWARD J. KRAMER† AND CHARLES L. BAUER

Department of Metallurgy and Materials Science, Carnegie Institute of Technology, Pittsburgh, Pennsylvania
(Received 12 May 1967)

Internal-friction and Young's-modulus measurements have been performed on as-grown and deformed niobium single crystals as a function of temperature and external magnetic field. The crystals are driven in longitudinal resonance between 1.5 and 10°K at 80 and 240 kHz. An internal-friction relaxation peak is observed at 3.24°K in the superconducting state, but shifts abruptly to 2.08°K when the mixed state is established. This peak is characterized by a single relaxation time τ , defined by the expression $\tau = \tau_0 \exp(E/kT)$. The activation energy E and the attempt frequency τ_0^{-1} , respectively, are 0.0019 eV and 6×10^9 rad/sec in the superconducting state, and 0.0016 eV and 4×10^9 rad/sec in the normal state (k is Boltzmann's constant and T denotes the absolute temperature). Effects of plastic deformation and residual-impurity content suggest that the relaxation process involves the motion of dislocations, modified by the presence of residual chemical impurities. Based on this premise, the interaction between dislocations and magnetic fluxoids is inferred to be attractive. Young's modulus also reflects the relaxation, and, in addition, decreases with decreasing temperature below 4°K. This decrease, however, is not consistent with ordinary relaxation mechanisms.

1. INTRODUCTION

THREE distinct thermodynamic states (excluding surface effects) are exhibited by type-II superconductors, depending on the strength of the external magnetic field H . When H is less than some lower critical field H_{c1} , the magnetic field is excluded from the bulk of the superconductor, and the superconducting state obtains everywhere. When H exceeds H_{c1} ,

however, partial penetration of the magnetic field occurs in the form of quantized lines of magnetic flux, hereafter termed fluxoids.¹⁻³ Since each fluxoid is characterized by a normal-like core, a mixed state composed of superconducting and normal material obtains. Finally, when H exceeds an upper critical field H_{c2} , the fraction of normal-like material becomes unity, and all superconducting properties vanish.

* Based on a dissertation prepared by E. J. Kramer in partial fulfillment of the requirements for the degree of Doctor of Philosophy at Carnegie Institute of Technology.

† Present address: Department of Materials Science and Engineering, Cornell University, Ithaca, New York.

¹ A. A. Abrikosov, *Zh. Eksperim. i Teor. Fiz.* **32**, 1442 (1957) [English transl.: *Soviet Phys.—JETP* **5**, 1174 (1957)].

² D. Cribier, B. Jacrot, B. Farnoux, and L. Madhav Rao, *J. Appl. Phys.* **37**, 952 (1966).

³ C. Caroli, P. G. DeGennes, and J. Matricon, *Phys. Letters* **9**, 370 (1964).

TABLE I. Estimated impurity content and orientation parameter Γ for the niobium specimens utilized in the present investigation. The parameter Γ is defined as $l^2m^2+m^2n^2+l^2n^2$ where l , m , and n denote the cosines of the angles circumscribing the specimen axis and the three $\langle 100 \rangle$ directions.

Specimen	Estimated impurity content (ppm)	$\Gamma(l,m,n)$
MRC (as-grown)	300	0.143
MRC (deformed)	300	0.143
BTL (deformed)	60	0.118

Experimental observations indicate that certain properties of type-II superconductors, e.g., the critical-current density and the degree of magnetic hysteresis, are affected significantly by metallurgical structure.⁴ Moreover, it is believed that the structure sensitivity is due primarily to the interaction of fluxoids with various lattice defects and impurities. These imperfections inhibit the motion of fluxoids, and thereby influence the response of the superconductor to electric and magnetic fields. The purpose of this research is to utilize internal-friction and Young's-modulus measurements in the kHz frequency range as tools to interrelate metallurgical structure to the properties of type-II superconductors. The study of nominally pure niobium is deemed most desirable, since it is the most easily purified elemental superconductor that displays type-II behavior.

The remainder of this paper is divided into four sections. The following section describes experimental procedures and techniques. Experimental results are presented in Sec. 3, and analyzed in terms of various atomic models in Sec. 4. Principal conclusions of this investigation are summarized in Sec. 5.

2. EXPERIMENTAL PROCEDURE AND TECHNIQUE

Two niobium single-crystal cylinders were obtained, respectively, from the Materials Research Corporation (MRC), Orangeburg, New York, and from Levinstein and Soden of the Bell Telephone Laboratories (BTL), Murray Hill, New Jersey. The ratio of the electrical resistance of the MRC crystal at room temperature to that at 4.2°K in a 10 kOe magnetic field is about 70, compared to 500 for the BTL crystal.⁵ The impurity content is estimated from these ratios to be about 300 ppm for the MRC crystal and 60 ppm for the BTL crystal, assuming that the electron scattering cross section of impurities in niobium is identical to that of interstitial oxygen and nitrogen in tantalum.⁶ The crystals were strained 3 percent in tension over a 1.25-in. gauge length. The axial orientation of each crystal, determined by the Laue back-reflection x-ray technique, is expressed by the param-

eter $\Gamma = l^2m^2 + m^2n^2 + l^2n^2$, where l , m , and n denote the cosines of the angles circumscribing the specimen axis and the three $\langle 100 \rangle$ directions. The aforementioned characteristics are summarized in Table I for easy reference.

Internal friction reported as the (logarithmic) decrement Δ and Young's modulus Y are measured by an ac bridge method.⁷ One arm of the bridge consists of a quartz piezoelectric transducer bonded to a niobium single-crystal cylinder of slightly smaller cross sectional area. The lengths of the quartz and niobium crystals are adjusted so that their fundamental longitudinal resonant frequencies are matched at approximately 80 kHz. This composite oscillator is illustrated in Fig. 1.

The quantity Δ is determined from the effective ac resistances of the quartz transducer R_q and composite oscillator R_c by the expression

$$\Delta = (R_c - R_q) / K m_s f, \quad (2.1)$$

where m_s denotes the specimen mass, f denotes the resonant frequency of the composite oscillator, and K is a constant determined empirically from an impedance-versus-frequency curve.⁸ Fractional modulus variations of the specimen ($\Delta Y/Y$) are related to fractional resonant-frequency variations of the composite oscillator ($\Delta f/f$) by the expression

$$(\Delta Y/Y) = 2(m_c/m_s)(\Delta f/f), \quad (2.2)$$

where m_c denotes the composite oscillator mass. (The

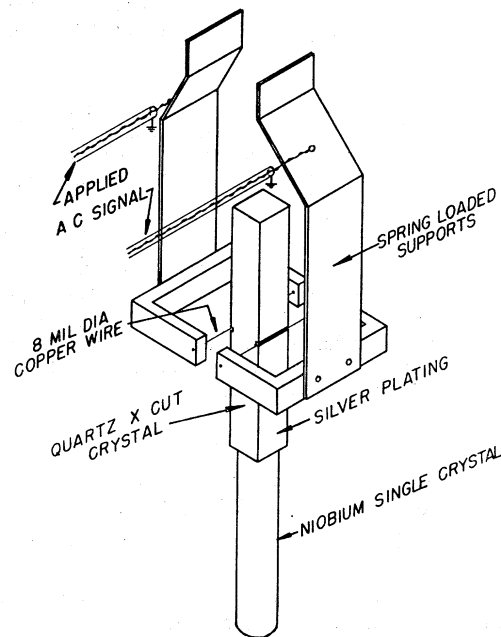


FIG. 1. Perspective illustration of the composite oscillator and support assembly.

⁴ J. D. Livingston and H. W. Shadler, *Progr. Mat. Sci.* **12**, 195 (1964).

⁵ H. J. Levinstein (private communication).

⁶ R. H. Chambers and J. Shultz, *Acta Met.* **10**, 466 (1962).

⁷ W. T. Cooke, *Phys. Rev.* **50**, 1158 (1936).

⁸ A. S. Nowick, *Phys. Rev.* **80**, 249 (1950).

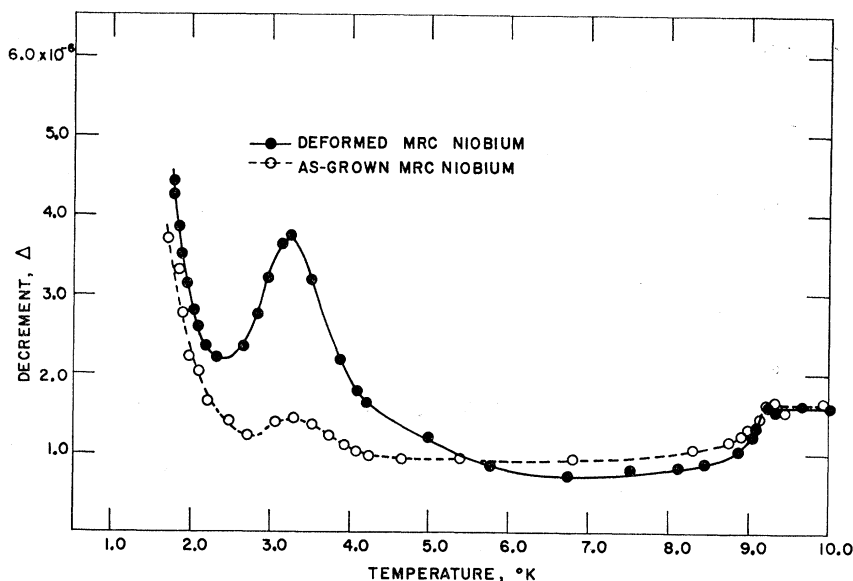


FIG. 2. Variation of the decrement Δ with absolute temperature in the superconducting state of both MRC specimens at 80 kHz. The absolute values of Δ have been adjusted so that the two curves coincide above the transition temperature (9.2°K).

quartz resonant frequency varies insignificantly below 10°K.) Variations in frequency of 0.2 ppm are detectable with the aid of a high-stability frequency synthesizer (General Radio model 1161A). All measurements are performed at a maximum strain amplitude of approximately 10^{-7} .

A conventional double-Dewar-flask system provides the low-temperature environment. The inner Dewar accommodates a double-walled specimen chamber centered within a superconducting solenoid so that the cylindrical axis of the specimen is aligned collinear with the magnetic field. The temperature of the chamber is controlled by adjusting the vapor pressure of the liquid-helium bath and the pressure of the exchange gas contained between the chamber walls. The temperature of the specimen is measured with a germanium resistance thermometer, and thermal equilibration is facilitated by introducing a few Torr of helium exchange gas into the innermost chamber.

3. EXPERIMENTAL RESULTS

A. Control Experiments

The values of Δ and $(\Delta Y/Y)$ often are biased by extraneous contributions, especially at low temperatures where the dissipation of energy is relatively small. The following control experiments are designed to insure that values reported herein are intrinsic characteristics of the niobium specimens.

Previous investigations indicate that variations of internal friction and elastic moduli with temperature and magnetic field, due to the quartz, bond material, and a few Torr of helium exchange gas are negligible below 10°K.^{9,10} Two experiments were performed

⁹ B. Welber and S. L. Quimby, *Acta Met.* **6**, 351 (1958).

¹⁰ D. F. Gibbons and C. A. Renton, *Phys. Rev.* **114**, 1257 (1959).

during the course of this investigation which provide similar evidence. The temperature and magnetic-field dependence of the internal friction and resonant frequency of the quartz transducer were measured, and it was found that Young's modulus of quartz does not vary in excess of 1 ppm when the temperature is varied between 10 and 1.5°K, or when H is increased to 10 kOe, or when the exchange gas pressure in the specimen chamber is varied below 1 Torr. The decrement remains constant from 10 to 5°K, and decreases slowly with decreasing temperature thereafter. A similar experiment, designed to measure extraneous contributions from the bond material (Duco cement), was performed with a composite oscillator composed of two identical quartz transducers. The variations of Δ and $(\Delta Y/Y)$ for this oscillator with temperature and magnetic field are equivalent to those measured with a solitary quartz transducer. Thus, it is concluded that the bond material does not affect the temperature dependence of Δ or $(\Delta Y/Y)$ below 10°K.

The absolute value of Δ for the quartz transducer is more sensitive to external influences. For example, the decrement varies as $4 \times 10^{-9} H^2$ (kOe)⁻², and decreases from 2×10^{-6} to 1×10^{-6} as the exchange-gas pressure is reduced from 1 to 0.1 Torr. Nevertheless, these variations are negligible compared to the magnitude of subsequent internal-friction measurements.

B. Temperature Dependence of Internal Friction

Variations of Δ with temperature for the as-grown and deformed MRC crystals in the absence of a magnetic field are depicted in Fig. 2. An abrupt decrease at 9.2°K marks the normal to superconducting transition of both crystals. However, an internal-friction peak centered at 3.24°K represents the most striking feature of these data. The peak height (relative

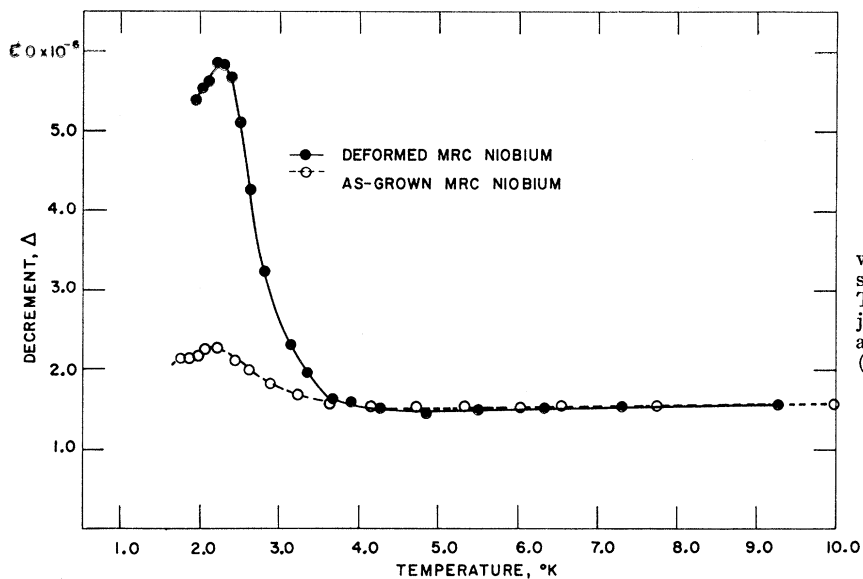


FIG. 3. Variation of the decrement Δ with absolute temperature in the normal state of both MRC specimens at 80 kHz. The absolute values of Δ have been adjusted so that the two curves coincide above the transition temperature (9.2°K).

FIG. 4. Variation of the decrement Δ with absolute temperature in the superconducting state of the deformed BTL specimen at 80 kHz (the ordinate is expanded near the transition temperature in the insert). The variation of Δ for the deformed MRC is indicated by the dashed line for comparison.

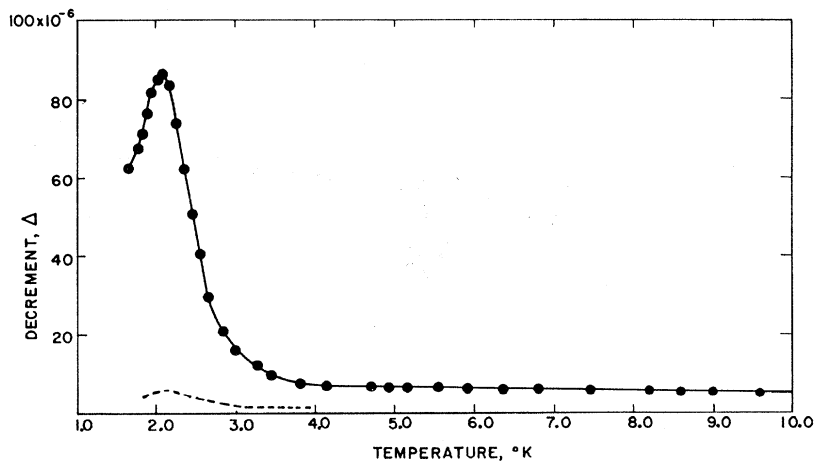
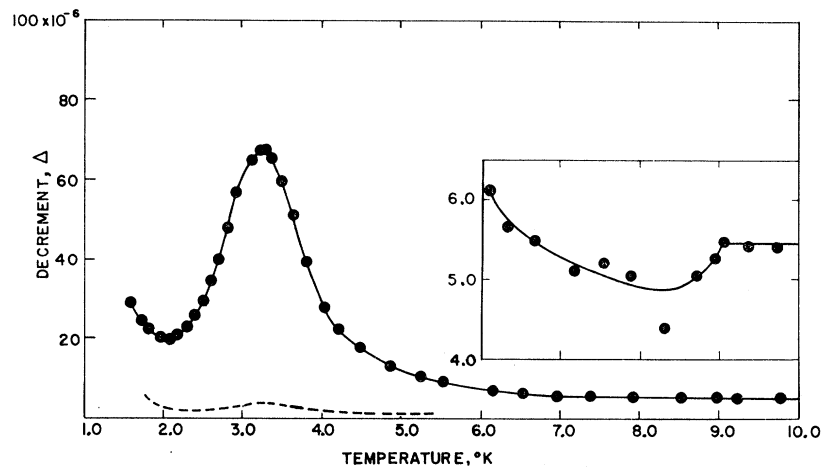


FIG. 5. Variation of the decrement Δ with absolute temperature in the normal state of the deformed BTL specimen at 80 kHz. The variation of Δ for the deformed MRC crystal is indicated by the dashed line for comparison.

to the background) in the deformed crystal exceeds that in the as-grown crystal by a factor of ten. Below 2.2°K, the internal friction of both crystals increases sharply, suggesting the presence of another internal-friction peak centered at a lower temperature.

The temperature dependence of Δ is altered when superconductivity is quenched by a magnetic field, as illustrated in Fig. 3. The abrupt decrease of Δ at 9.2°K observed in the superconducting state is absent in the normal state, and an internal-friction peak now is centered at 2.08°K. The peak height in the deformed crystal exceeds that in the as-grown crystal by a factor of ten, and the ratio of normal to superconducting peak height is 4:3 for the deformed crystal. The temperature dependence of Δ in the normal state is not affected by application of magnetic fields up to 40 kOe (although the background is raised). Thus, the normal-state peak cannot be associated with surface superconductivity.

In order to determine the effect of residual impurities on the internal-friction peaks, the deformed BTL crystal was investigated. The temperature dependence of Δ for this crystal in the superconducting and normal states is illustrated in Figs. 4 and 5, respectively. The variation of Δ for the deformed MRC crystal is indicated by the dashed line for comparison. Although the internal-friction peaks are enhanced by more than an order of magnitude, they are centered at the same temperatures as those of MRC crystal and are characterized by the same ratio of normal to superconducting peak height. The fact that this ratio is unaltered in crystals of dissimilar impurity content and origin suggests that the peaks are manifestations of the same process.

Perhaps a more relevant indication of the purity of the MRC and BTL crystals is provided by the location and height of the α peak (a deformation-induced internal-friction peak), since Chambers and co-workers have shown that this peak increases in height and shifts to higher temperatures as interstitial impurities are removed from the vicinity of dislocations.^{6,11} The α peaks of the deformed MRC and BTL crystals are compared in Fig. 6. Although both crystals were deformed similarly, it appears that the dislocations in the BTL crystal are significantly "cleaner" than those in the MRC crystal. Thus, observations of the α peak are consistent with the estimated impurity contents reported in Table I.

Since the general appearance of the internal-friction peaks displayed in Figs. 2 through 5 is indicative of a relaxation process, the frequency dependence of the peak position was investigated. The third harmonic (240 kHz) was excited in the BTL crystal, and it was observed that the superconducting-state peak shifts to 3.75°K, and the normal-state peak shifts to 2.37°K. If the proposed relaxation process is characterized by a

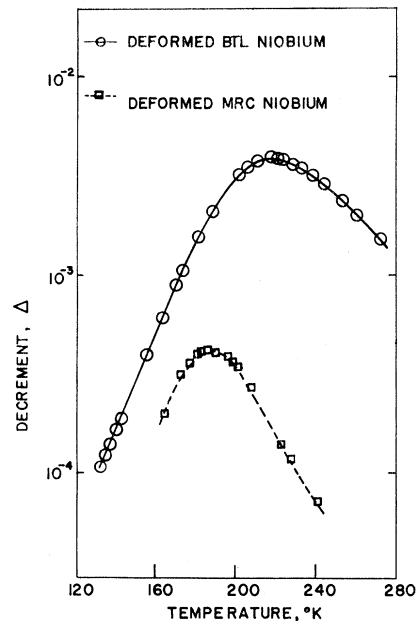


FIG. 6. Location of the α peak in the deformed (3 percent in tension) MRC and BTL crystals. The α peak increases in height and shifts to higher temperatures as interstitial impurities are removed (see Refs. 6 and 11).

single relaxation time τ , given by the expression

$$\tau = \tau_0 \exp(E/kT), \quad (3.1)$$

where k is Boltzmann's constant and T denotes the absolute temperature, the activation energies E and the attempt frequencies τ_0^{-1} can be determined from the temperature shift of the peak maximum. By equating $2\pi f\tau$ to unity at this temperature in the superconducting state, E and τ_0^{-1} are computed to be 0.0019 ± 0.0002 eV and 6×10^8 rad/sec, respectively. In the normal state, E and τ_0^{-1} are computed to be 0.0016 ± 0.0002 eV and 4×10^9 rad/sec, respectively.

The heights of the internal friction peaks Δ_m in the BTL crystal are greater at the third harmonic. In the superconducting state Δ_m is enhanced from 6.2×10^{-5} at 80 kHz to 9.0×10^{-5} at 240 kHz. In the normal state Δ_m is enhanced similarly by 50 percent, from 8.2×10^{-5} at 80 kHz to 12×10^{-5} at 240 kHz, and thus the 4:3 ratio of normal-to-superconducting peak height is maintained. The increase in peak height with frequency is of doubtful significance, however, since multiple harmonics excite different portions of the specimen.

The reciprocal temperature width of the internal-friction peaks at half-maximum $w(1/T)$ can be compared with the theoretical width for a process characterized by a single relaxation time¹²; viz.,

$$w(1/T) = (k/E) \ln[(2+\sqrt{3})/(2-\sqrt{3})]. \quad (3.2)$$

¹¹ R. H. Chambers, *Physical Acoustics*, edited by W. P. Mason (Academic Press Inc., New York, 1966), Vol. IIIA, Chap. 4.

¹² A. S. Nowick, in *Progress in Metal Physics*, edited by B. Chalmers (Interscience Publishers, Inc., New York, 1953), Vol. 4.

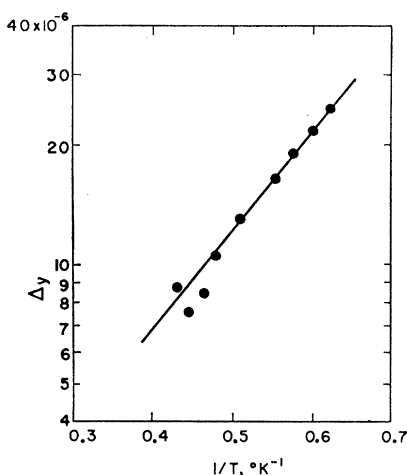


FIG. 7. Logarithm of the decrement caused by the y relaxation $\log \Delta_y$ versus the reciprocal absolute temperature $1/T$.

Equation (3.2) yields a value of 0.119°K^{-1} in the superconducting state compared to an observed value of 0.100°K^{-1} , whereas it yields a value of 0.142°K^{-1} in the normal state compared to an observed value of 0.144°K^{-1} . Considering the uncertainty of measured values of E , it is concluded that a single relaxation process can account for experimental observations. This process is termed the x relaxation process.

The decrement associated with a relaxation process characterized by a single relaxation time is given by the expression¹²

$$\Delta = \pi \delta \omega \tau / (1 + \omega^2 \tau^2), \quad (3.3)$$

where ω denotes the applied angular frequency and $\delta = \Delta_m / \pi$ denotes the relaxation strength. Empirically, it is found that Eq. (3.3), with the appropriate values of δ , τ_0 , and E , can reproduce the experimental temperature dependence of Δ except in the superconducting

state below 2.5°K . It is believed that disagreement is due to another thermally activated relaxation process. This process is termed the y relaxation process.

The internal friction due to the y relaxation process is isolated by subtracting the computed x relaxation curve and the background decrement from the experimental data. The decrement due to the high-temperature extremity of the y relaxation peak is approximated by neglecting the second term in the denominator of Eq. (3.3). Therefore, $\delta\tau_0$ and E can be determined from the intercept and slope, respectively, of a plot of $\log \Delta$ versus $1/T$, as depicted in Fig. 7. From this plot, E and $\delta\tau_0$ are computed to be 0.0005 eV and 4×10^{-13} sec/rad, respectively.

Although the annealing characteristics of the x and y relaxation peaks were not studied explicitly, it was observed that the peaks are not affected noticeably by a room-temperature anneal of several months.

C. Magnetic-Field Dependence of Internal Friction

The decrement changes abruptly when niobium transforms from the superconducting state to the mixed state at H_{c1} . Figure 8 depicts Δ as a function of H at three temperatures near the x relaxation peak for the deformed MRC crystal. The sudden decrease that occurs as the mixed state is established is due either to the disappearance or shift of the x relaxation peak. To distinguish between these two possibilities, H was increased from 0 to 1.65 kOe at 3.3°K (to allow flux penetration), and subsequently Δ was measured as a function of T . In this case, a relaxation peak characterized by the normal-state values of E , τ_0 , and δ appears at the same temperature as that of the normal-state peak. Thus, it is concluded that E and δ shift from their values in the superconducting state to those in the normal state soon after the mixed state is

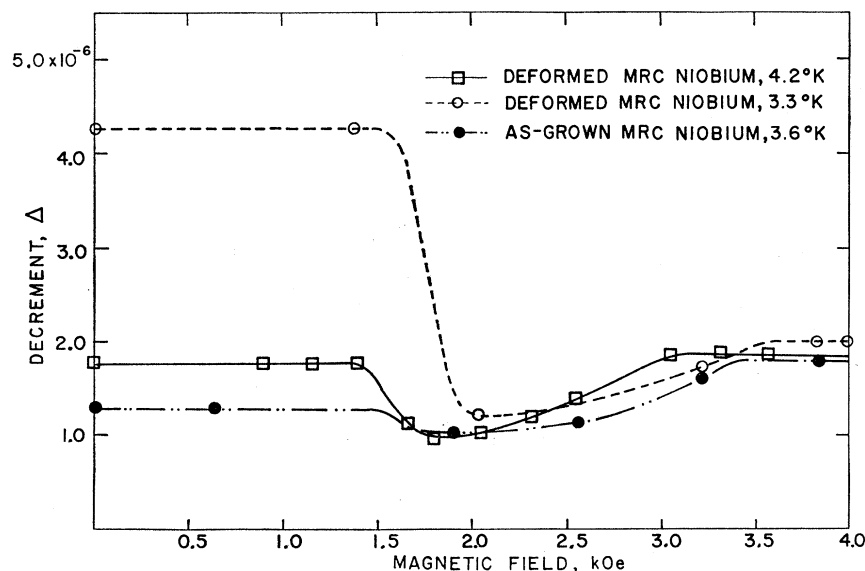
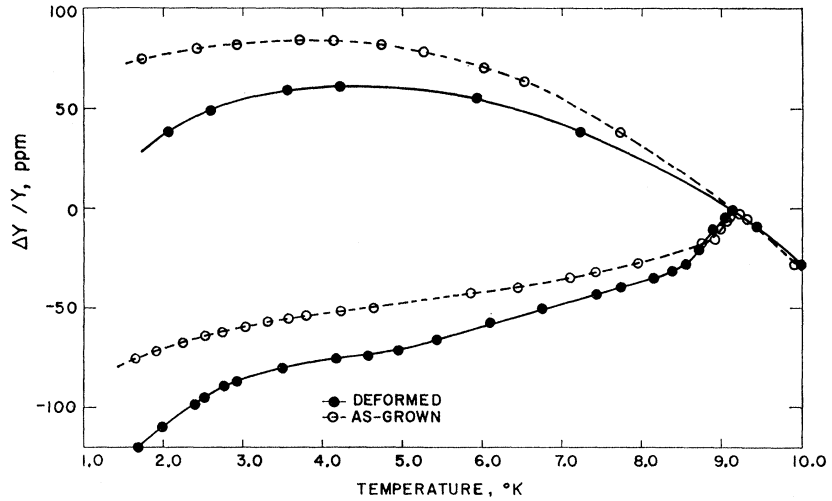


FIG. 8. Variation of the decrement with external magnetic field for the MRC specimens at various temperatures near the x relaxation peak.

FIG. 9. Variation of the relative Young's modulus ($\Delta Y/Y$) with absolute temperature in the superconducting (lower curves) and normal (upper curves) states of both MRC specimens at 80 kHz. The reference temperature is chosen arbitrarily to be 9.2°K.



established. The subsequent increase in Δ with increasing H is about equal to the increase of internal friction that accompanies the superconducting to normal transition.

D. Temperature Dependence of Young's Modulus

Variations of the relative Young's modulus with temperature, designated $(\Delta Y/Y)_s$ and $(\Delta Y/Y)_n$ in the superconducting and normal states, respectively, are depicted in Figs. 9 and 10. Figure 10 also includes Young's-modulus variations measured at the third harmonic of the composite oscillator (240 kHz). The reference temperature is chosen arbitrarily to be 10°K. An abrupt divergence between $(\Delta Y/Y)_s$ and $(\Delta Y/Y)_n$ at 9.2°K marks the normal-to-superconducting transition at the fundamental frequency and the third harmonic. In addition, a contribution to $(\Delta Y/Y)$

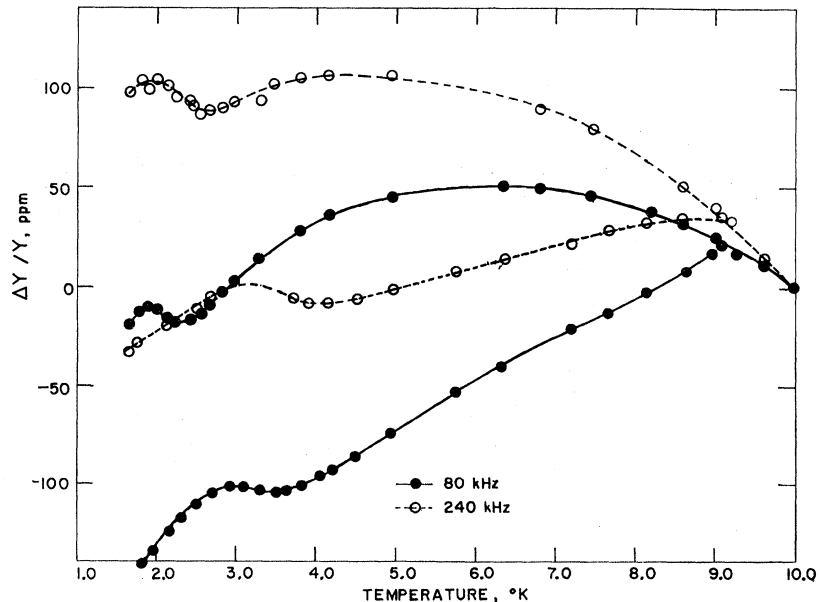
associated with the α relaxation is superposed on a gradual decrease of $(\Delta Y/Y)$ with decreasing temperature.

The modulus variation associated with the α relaxation is given by the expression¹²

$$(\Delta Y/Y) = \delta / (1 + \omega^2 \tau^2). \tag{3.4}$$

When the computed values of Eq. (3.4) are subtracted from the experimental curves for the BTL crystal depicted in Fig. 10, the residue decreases smoothly through the temperature regions of the α relaxation peaks as illustrated in Fig. 11, providing further evidence that the α relation is characterized by single relaxation times. The changes of Young's modulus due to the α relaxation in the deformed MRC crystal cannot be resolved, since the total modulus increase is computed from the α peak height to be only

FIG. 10. Variation of the relative Young's modulus ($\Delta Y/Y$) with absolute temperature in the superconducting (lower curves) and normal (upper curves) states of the deformed BTL crystal at 80 and 240 kHz. The reference temperature is chosen arbitrarily to be 10.0°K.



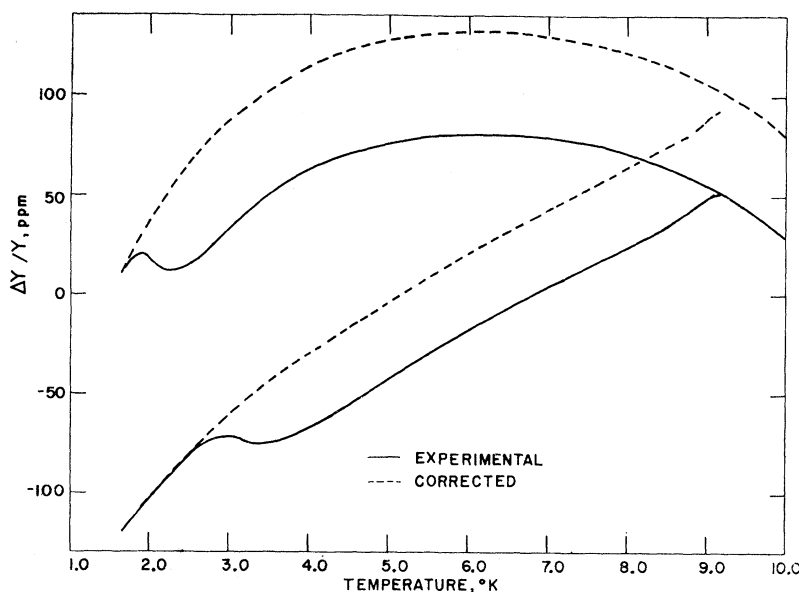


FIG. 11. Variation of the relative Young's modulus ($\Delta Y/Y$) with absolute temperature in the superconducting (lower curves) and normal (upper curves) states of the deformed BTL crystal at 80 kHz. The solid curves are reproduced from Fig. 10, whereas the dashed curves are corrected so as to eliminate the α relaxation contribution.

1.9 ppm in the superconducting state, and 2.6 ppm in the normal state. The α relaxation modulus change is, of course, even smaller for the as-grown MRC crystal.

E. Magnetic-Field Dependence of Young's Modulus

Figure 12 illustrates ($\Delta Y/Y$) as H is cycled from zero to above H_{c2} and back to zero. The curve for ascending fields virtually is independent of H below H_{c1} (1.2 kOe) and above H_{c2} (3.0 kOe), whereas the mixed state is characterized by a rapid rise during the first 0.4 kOe and a linear variation thereafter. The curve for descending fields varies linearly from H_{c2} to 1.0 kOe, and then becomes nearly independent of H . The remanent ($\Delta Y/Y$) of 23 ppm can be obliterated by warming the specimen above its transition temperature. Further details and discussion of the magnetic field dependence of ($\Delta Y/Y$) are presented elsewhere.¹³

4. DISCUSSION

A. α and γ Relaxation Mechanisms

Any model which is utilized to interpret the α and γ relaxation peaks in terms of atomic mechanisms must account for the following observations:

- All available evidence indicates that the peaks are manifestations of relaxation processes characterized by single and unique relaxation times.
- The peaks are enhanced by plastic deformation.
- Peak enhancement by plastic deformation is greatest in the purest specimen.
- The peaks shift abruptly when the mixed state is established.
- The temperature of the peak maxima is unaffected by nominal impurity content (in contrast to the α peak).

(f) The peaks are stable with respect to room-temperature anneals of several months.

The complex series of attenuation peaks observed by Claiborne and Einspruch at MHz frequencies in the superconducting state of a variety of polycrystalline type-I and type-II materials¹⁴⁻¹⁸ do not seem to be related to the α and γ peaks. The amplitudes of the attenuation peaks are increased by plastic deformation, decreased by annealing, and disappear entirely when the mixed state is established. The α and γ relaxations, however, are observed in the superconducting, mixed, and normal states. Moreover, the predicted shift of each attenuation peak with frequency is contrary to that measured for the α and γ relaxations.

The aforementioned observations also seem to rule out an isolated chemical impurity relaxation, such as observed in iron,^{19,20} since the relaxation strength decreases with increasing impurity content. Likewise, isolated debris caused by plastic deformation cannot give rise to the observed results, since specimens subjected to equivalent deformations exhibit relaxation strengths that vary by an order of magnitude. The above observations do, however, suggest that an atomic process involving the motion of dislocations, modified by the presence of residual chemical impurities, is responsible for the relaxations. Final

¹⁴ L. T. Claiborne and N. G. Einspruch, Phys. Rev. Letters **10**, 49 (1963).

¹⁵ L. T. Claiborne and N. G. Einspruch, Phys. Rev. **132**, 621 (1963).

¹⁶ L. T. Claiborne, T. Olsen, and N. G. Einspruch, in Proceedings of Conference on Physics of Type-II Superconductivity, Cleveland, Ohio, 1964 (unpublished).

¹⁷ L. T. Claiborne and N. G. Einspruch, Phys. Letters **8**, 160 (1964).

¹⁸ L. T. Claiborne and N. G. Einspruch, J. Appl. Phys. **37**, 925 (1965).

¹⁹ L. C. Weiner and M. Gensamer, Acta Met. **5**, 692 (1957).

²⁰ T. S. Kê, Trans. AIME **176**, 448 (1948).

¹³ E. J. Kramer and C. L. Bauer, Phys. Status Solidi **22**, 199 (1967).

judgement, of course, must await further studies concerning the effects of chemical impurities, prestrain, and heat treatment in a variety of materials.

Most dislocation-relaxation mechanisms are characterized by a spectrum of relaxation times. For example, the relaxation time for diffusive motion of geometrical kinks is dependent on the separation between impurity pinning points.²¹ Since pinning points usually distribute randomly along dislocations, a spectrum of relaxation times will result. The generation of thermal (double) kinks originally was assumed to give rise to a relaxation process characterized by a single relaxation time²²; however, recent calculations indicate that the relaxation is broadened by reverse jumps of kinks²³ and internal-stress fields.²³⁻²⁵

One of the few dislocation mechanisms that, in principle, can account for a single and unique relaxation time involves thermally activated motion of partial dislocations in the stress field of pinning points.²⁶ In this case, the activation energy is dependent on the binding energy of the pinning point to an edge dislocation and the separation between the partial dislocations. Qualitatively, at least, this model can account for experimental observations. Assuming that a single pinning species is active, δ is predicted to be

proportional to the product of the squared-mean free-dislocation-segment length L^2 and the number of defect-dislocation complexes Δc , where c denotes the concentration of defects along the dislocation and Δ denotes the dislocation density. When the mean separation between pinning points is less than the separation between dislocation nodes, L^2 is proportional to $1/c^2$ and δ increases with increasing Δ and decreasing c in agreement with experimental observations. The α and γ relaxations could arise from dissimilar pinning-point species or locations near the dislocation core. Moreover, the shift in τ from the superconducting to normal-state value could be due to the change in the binding energy of the defect, but a calculation of the magnitude and direction is not feasible, since the defect probably resides within the dislocation core. In fact, the entire model is suspect until the atomic configuration of the dislocation core and the change in stacking-fault energy due to the superconducting to normal-state transition are known in some detail. Nevertheless, a systematic study of the effect of hydrogen (and other interstitial impurities) would provide some indication of the correctness of this model.

The fact that the α and γ relaxations assume their normal state characteristics abruptly when the mixed state is established implies that the relaxing entities always reside in normal-state regions of the mixed state. An attractive interaction between fluxoids and dislocations could produce a normal-state environment, since the (normal) fluxoid cores would lie preferentially along dislocations. The first-order dislocation-fluxoid elastic interaction²⁷ and the interaction due to a reduction of the electron mean free path near the dislocation²⁸ are attractive; the former, however, gives rise to a fluxoid equilibrium position which does not coincide with the dislocation core. Thus, the electron-mean-free-path interaction may provide the bulk of the attractive force if the relaxing entities are situated within the core of edge dislocations.

B. Temperature Dependence of Young's Modulus

All elastic moduli must approach absolute zero with zero slope.²⁹ Moreover, the approach usually is characterized by negative curvature. The Young's-modulus curves of the normal state of all three niobium crystals are deemed anomalous in this respect. The strength of the anomaly can be characterized by either of two parameters: $d(\Delta Y/Y)_n/dT$ at a fixed low temperature (2°K) or the temperature T_m corresponding to the maximum value of $(\Delta Y/Y)_n$. These parameters, obtained from Figs. 9 and 11, are listed in Table II. The strength of the anomaly is larger in the deformed crystals, smaller in the impure crystals, and smaller at

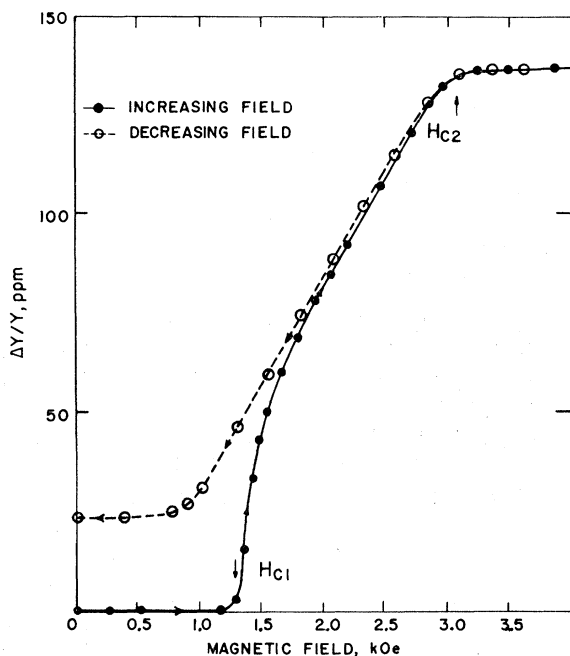


FIG. 12. Variation of the relative Young's modulus ($\Delta Y/Y$) at 4.2°K, relative to that measured in the absence of magnetic field H , with increasing and decreasing H for the deformed MRC specimen at 80 kHz. The lower and upper critical field, H_{c1} and H_{c2} , respectively, are designated by arrows.

²¹ A. D. Brailsford, Phys. Rev. **122**, 778 (1961); **128**, 1033 (1962).

²² A. Seeger, Phil. Mag. **1**, 651 (1956).

²³ V. K. Paré, J. Appl. Phys. **32**, 332 (1961).

²⁴ A. D. Brailsford, Phys. Rev. **137**, A1562 (1965).

²⁵ R. J. Arsenault, Acta Met. **15**, 501 (1967).

²⁶ L. J. Bruner, Phys. Rev. **118**, 399 (1960).

²⁷ E. J. Kramer and C. L. Bauer, Phil. Mag. **15**, 1189 (1967).

²⁸ A. V. Narlikar and D. Dew Hughes, Phys. Status Solidi **6**, 383 (1964).

²⁹ H. B. Huntington, in *Solid State Physics*, edited by F. Seitz and D. Turnbull (Academic Press Inc., New York, 1958), Vol. **7**, p. 214.

TABLE II. Parameters characterizing the strength of the anomalous modulus decrease. The quantity T_m denotes the temperature corresponding to the maximum value of $(\Delta Y/Y)_n$, and $d(\Delta Y/Y)_n/dT$ denotes the temperature derivative of Young's modulus at 2°K .

Specimen	T_m ($^\circ\text{K}$)	$d(\Delta Y/Y)_n/dT$ (ppm/ $^\circ\text{K}$)	Frequency (kHz)
As-grown (MRC)	4.0	10	80
Deformed (MRC)	4.5	30	80
Deformed (BTL)	6.4	70	80
Deformed (BTL)	4.5	20	240

the higher frequency, suggesting that the anomaly is due to defect motion. Modulus decreases with decreasing temperature have been observed previously in niobium,³⁰ but were attributed to changes in bonding between atoms.³¹ However, it seems improbable that the effects of frequency, purity, and deformation observed in this study can be explained entirely by such changes.

In principle, a transition from the adiabatic Young's modulus Y_a to the isothermal Young's modulus Y_i can give rise to a modulus decrease. The total decrease is given by the expression³²

$$(Y_a - Y_i)/Y = (\alpha^2 T / \rho C_v) Y, \quad (4.1)$$

where α denotes the linear coefficient of expansion, C_v denotes the specific heat per g mole, and ρ denotes the molar density. Utilizing the material parameters of niobium listed in Table III, Eq. (4.1) is evaluated to be 0.0057 ppm at 2°K . This magnitude is much too small to account for the observed variation of $(\Delta Y)/Y$. In Appendix A it is demonstrated that temperature gradients along the length of the specimen cannot give rise to the temperature dependence of $(\Delta Y)/Y$, since the magnitude is small compared with the ob-

TABLE III. Some material constants for niobium at 2°K .

Material constant and symbol	Value	Reference
Linear thermal expansion coefficient, α	$6.2 \times 10^{-9} (\text{K})^{-1}$	a
Young's modulus, Y	$12.65 \times 10^{11} \text{ dyn cm}^{-2}$	b
Molar density in superconducting state, ρ	$0.0921 \text{ g mole cm}^{-3}$	c
Specific heat in normal state, C_v	$0.0186 \text{ J/mole } ^\circ\text{K}$	d

^a H. M. Rosenberg, *Low Temperature Solid State Physics* (Oxford University Press, London, 1963), Table 2.1, p. 41; G. K. White (private communication).

^b Reference 35.

^c *Handbook of Chemistry and Physics*, edited by Charles D. Hodgman et al. (Chemical Rubber Publishing Company, Cleveland, Ohio, 1955), 37th ed., p. 374.

^d A. Brown, M. W. Zemansky, and H. A. Boorse, *Phys. Rev.* **92**, 52 (1953).

³⁰ K. J. Carroll, *J. Appl. Phys.* **36**, 3689 (1965).

³¹ F. H. Featherston and J. R. Neighbors, *Phys. Rev.* **130**, 1324 (1963).

³² W. P. Mason, *Physical Acoustics and the Properties of Solids* (D. Van Nostrand Company, Inc., 1958) p. 200.

served value and $(\Delta Y/Y)$ is expected to *increase* with decreasing temperature. Consideration of dimensional changes of the specimen lead to similar conclusions.

The gradual decrease of Young's modulus with decreasing temperature could reflect the high temperature extremity of a broad relaxation process. Such a relaxation is predicted by the Koehler-Granato-Lücke string model of a dislocation intermittently pinned by point defects.^{33,34} For an overdamped system, a modulus variation identical to Eq. (3.4) is predicted. The relaxation time τ for this process is given by

$$\tau = BL^2/\pi^2\gamma, \quad (4.2)$$

where B and γ denote the dislocation-damping constant and line tension, respectively. Thus, since B decreases with decreasing temperature, it is possible that Δ will increase and that $(\Delta Y/Y)$ will decrease. However,

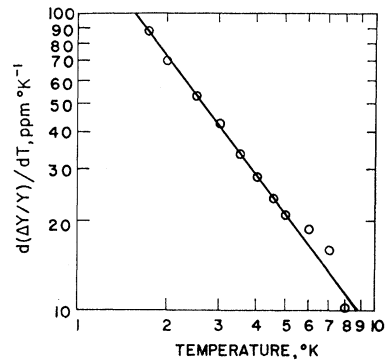


FIG. 13. Logarithm of $d(\Delta Y/Y)/dT$ versus logarithm of the absolute temperature. The quantity $(\Delta Y/Y)$ denotes the difference between the normal state Young's modulus measured at 80 kHz in the deformed BTL crystal and the modulus determined by fitting a parabolic curve to the normal state Young's modulus in the same crystal measured at 240 kHz between 4° and 10°K .

when reasonable values are substituted into Eq. (4.2), τ is determined to be approximately 10^{10} sec. The agreement is even worse if a model of a dislocation vibrating within its Peierls well is considered.

A generalized relaxation controlled by the dislocation-damping constant now is investigated by expressing the temperature dependence of B as

$$B = B_0 T^q, \quad (4.3)$$

where B_0 and q are positive constants. The fractional variation of Young's modulus at the high-frequency extremity of the relaxation ($\omega\tau > 1$) is obtained by combining Eqs. (3.4), (4.2), and (4.3) to yield

$$(\Delta Y/Y) = \delta(\pi^2\gamma/\omega B_0 L^2)^2 T^{-2q}, \quad (4.4)$$

where $(\Delta Y/Y)$ is taken from the experimental data as the difference between the normal state Young's

³³ J. S. Koehler, *Imperfections in Nearly Perfect Crystals* (John Wiley & Sons, Inc., New York, 1952), Chap. VII.

³⁴ A. Granato and K. Lücke, *J. Appl. Phys.* **27**, 583 (1956).

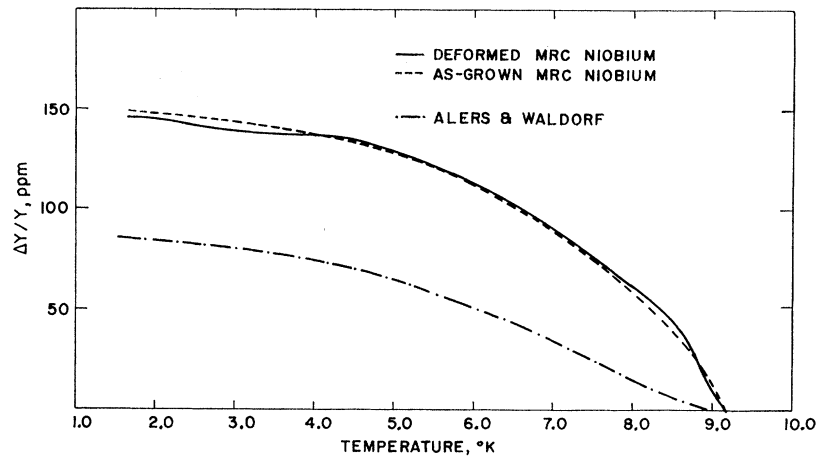


FIG. 14. The increment of Young's modulus between the superconducting and normal states $(\Delta Y/Y)_{sn}$, corrected for the x and y relaxations with the aid of Eq. (3.4), versus absolute temperature for both MRC specimens at 80 kHz. The results of Alers and Waldorf (Ref. 35) are indicated for comparison.

modulus measured at 80 kHz in the deformed BTL crystal and the Young's modulus determined by fitting a parabolic curve to the normal-state Young's modulus measured at 240 kHz between 4 and 10°K. (The results are qualitatively the same if the normal-state Young's modulus calculated from the data of Alers and Waldorf³⁵ is used as a standard.) Thus, a plot of $\log[d(\Delta Y/Y)_n/dT]$ versus $\log T$ should yield a straight line with a slope of $-(2q+1)$. The results are displayed in Fig. 13 where it is seen that the experimental points do fall on a straight line of slope -1.32 , and consequently q is equal to 0.16. However, all mechanisms for damped dislocation motion whose temperature dependence has been analyzed yield a damping constant that depends on temperature to the first power or higher.³⁶⁻³⁸ Furthermore, the decrement accompanying the Young's modulus change, given by the expression

$$\Delta = (\pi T/2q)\omega r d(\Delta Y/Y)/dT, \quad (4.5)$$

is estimated to be greater than 10^{-3} , whereas the

decrement that cannot be accounted for by either the x or y relaxations is less than 10^{-5} . Therefore, a simple relaxation model cannot explain the anomalous temperature dependence of Young's modulus.

The increment of Young's modulus between the superconducting and normal states $(\Delta Y/Y)_{sn}$, corrected for the x and y relaxations with the aid of Eq. (3.4), is plotted versus temperature in Figs. 14 and 15 for the MRC and BTL crystals, respectively. All measured values of $(\Delta Y/Y)_{sn}$ are nearly identical; however, they are not in agreement with the values computed in Appendix B from the data of Alers and Waldorf.³⁵ The discrepancy is probably not due to different anomalous modulus decrease strengths in the normal and superconducting states, since the as-received and deformed MRC crystals display identical variations of $(\Delta Y/Y)_{sn}$.

A clue to the possible cause of the elastic moduli discrepancy lies in the correction that is necessary to eliminate the effects of the x relaxation. The measured value of $(\Delta Y/Y)_{sn}$ for the BTL crystal is less than the

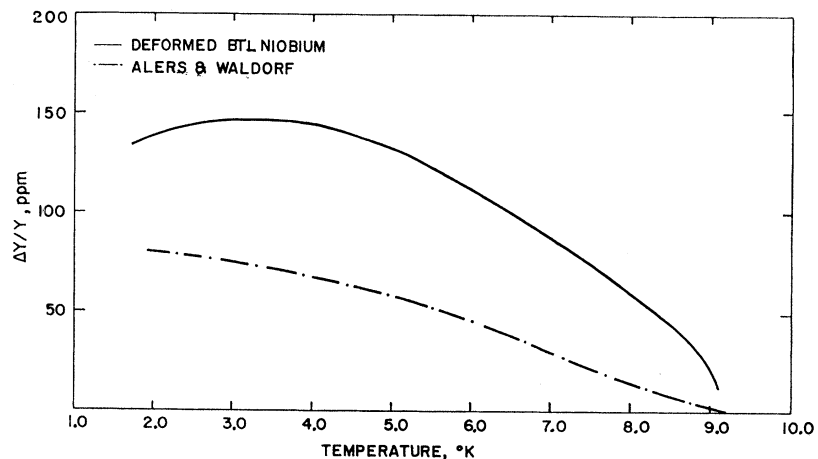


FIG. 15. The increment of Young's modulus between the normal and superconducting states $(\Delta Y/Y)_{sn}$, corrected for the x relaxation with the aid of Eq. (3.4), versus absolute temperature for the deformed BTL specimen at 80 kHz (the equivalent increment at 240 kHz is identical). The results of Alers and Waldorf (Ref. 35) are indicated for comparison.

³⁵ G. A. Alers and D. L. Waldorf, IBM J. Res. Develop. 6, 89 (1962).

³⁶ G. Leibfried, Z. Physik 127, 344 (1950).

³⁷ J. Lothe, J. Appl. Phys. 33, 2116 (1962).

³⁸ W. P. Mason, J. Acoust. Soc. Am. 32, 458 (1960).

corrected value at temperatures above the α relaxation because δ is greater in the normal than in the superconducting state. Other relaxations, likewise, could affect measured values. For example, if the sum of all the relaxation strengths of all lower-temperature relaxations in the superconducting state exceeds the sum of relaxation strengths in the normal state by 80 ppm for the deformed BTL crystal and by 60 ppm for the MRC crystals, the discrepancy between the data of Alers and Waldorf and the present measurements would be eliminated.

There is support for the idea that relaxations (in addition to the γ relaxation) exist below 2.0°K at 80 kHz in niobium. Alers and Waldorf³⁹ observed an increase in $\frac{1}{2}(C_{11}-C_{12})$, of 40 ppm at 10 MHz below 2.5°K in the superconducting state of an impure as-grown niobium crystal, which is reduced to about 8 ppm by annealing. This (inferred) relaxation process will occur below 2°K at a frequency of 80 kHz. The prevalent lack of agreement between specimens of disparate impurity content and origin^{9,10,40,41} could be due to similar relaxation phenomena.

5. SUMMARY

An internal-friction relaxation peak in niobium is observed at 3.24°K in the superconducting state, but shifts abruptly to 2.08°K when the mixed state is established. This peak is characterized by a single relaxation time τ in which the activation energy and attempt frequency, respectively, are 0.0019 eV and 6×10^8 rad/sec in the superconducting state, and 0.0016 eV and 4×10^9 rad/sec in the normal state. The increase in Δ below the α relaxation temperature in the superconducting state is attributed to the γ relaxation process, characterized by an activation energy of 0.0005 eV. Effects of plastic deformation and residual impurity content suggest that the α relaxation process involves the motion of dislocations, modified by the presence of residual chemical impurities. Based on this promise, the interaction between dislocations and magnetic fluxoids is inferred to be attractive.

The corrected Young's modulus decreases with decreasing temperature below 4.0°K in both normal and superconducting states for all specimens. The strength of this decrease is enhanced by deformation and reduced by impurity additions. Interpretation of the results in terms of a generalized mechanism of dislocation relaxation controlled by a damping constant gives rise to two inconsistencies: First, a small temperature dependence of B is computed from the data, and second, concomitant values of Δ are not observed. Moreover, specific models of damping-constant controlled dislocation relaxations predict unlikely mag-

nitudes of the damping constant and/or the average dislocation loop length between pinning points.

Finally, the internal-friction increment between the superconducting and normal states differs by a factor of two with the results of Alers and Waldorf. The disparity in α relaxation strength between the normal and superconducting state encourages the speculation that at least part of the discrepancy is due to lower temperature (<2°K) relaxations.

6. ACKNOWLEDGMENTS

The authors would like to express their appreciation to the U. S. Atomic Energy Commission for support of the present research and to H. J. Levinstein and R. Soden for the preparation and use of a niobium single crystal. One of the authors (E. J. K.) also received partial financial support during the course of this investigation in the form of a Fellowship from the National Science Foundation.

APPENDIX A: TEMPERATURE DEPENDENCE OF YOUNG'S MODULUS IN THE PRESENCE OF A TEMPERATURE GRADIENT

The compliance, $S_{11} \equiv 1/Y$, as determined from the resonant frequency of an inhomogeneous bar of length l is determined by the average of the local compliances $S_{11}(x)$ according to the formula⁸

$$S_{11} = (2/l) \int_0^l S_{11}(x) \sin^2(\pi x/l) dx, \quad (A1)$$

where x denotes the distance along the bar. If the temperature is known for all x , and the temperature dependence of the compliance is known, the effect of a temperature gradient of S_{11} can be calculated from Eq. (A1).

When one end of the bar is fixed at a temperature T_0 and the other end is exposed to a constant heat input Q , a temperature distribution $T(x)$ results. The differential equation that governs $T(x)$ is

$$dT/dx = Q/AK(T), \quad (A2)$$

where $K(T)$ denotes the thermal conductivity, which is equal to βT in the normal state below 7°K,⁴¹ and A denotes the cross-sectional area of the bar. The temperature distribution that results is

$$T^2 = T_0^2 + (2Q/A\beta)x. \quad (A3)$$

The compliance of the normal state varies with temperature as³⁸

$$1/S_{11}(T) = (1 - aT^2)/S_{11}(0), \quad (A4)$$

where $S_{11}(0)$ is the compliance at absolute zero and a is a constant. Combination of Eqs. (A1), (A3), and (A4) yields

$$S_{11}(T_0) = [2S_{11}(0)/l] \int_0^l \frac{\sin^2(\pi x/l) dx}{1 - aT_0^2 + (2aQ/A\beta)x}. \quad (A5)$$

³⁹ G. A. Alers (private communication).

⁴⁰ J. K. Landauer, Phys. Rev. **96**, 296 (1954).

⁴¹ W. P. Mason and H. E. Bommel, J. Am. Acoust. Soc. **28**, 930 (1956).

The temperature dependence of Young's modulus $(1/Y)(dY/dT_0)$ then is given by the expression

$$(1/Y)(dY/dT_0) = -[1/S_{11}(0)][\partial S_{11}(T_0)/\partial T_0] \\ = (-4aT_0/l) \int_0^l \frac{\sin^2(\pi x/l) dx}{[1-aT_0^2 - (2aQ/A\beta)x]^2}. \quad (\text{A6})$$

When values of $\beta = 0.10 \text{ W}^\circ\text{K}^{-2} \text{ cm}^{-1}$,⁴² $a = 10^{-6} \text{ }^\circ\text{K}^{-2}$,³⁵ $l = 2.25 \text{ cm}$, $A = 0.15 \text{ cm}^2$, and $Q = 1 \text{ W}$ are substituted into Eq. (A6), the second and third terms in the denominator are found to be small compared to unity. The denominator, therefore, is given by the first term in a binomial expansion and Eq. (A6) reduces to

$$(1/Y)(dY/dT_0) = -2aT_0[1 + 2a(T_0^2 + Ql/A\beta)]. \quad (\text{A7})$$

Since all terms contained within the square brackets are positive, the slope of Young's modulus with temperature is always negative. Therefore, a maximum in the measured Young's modulus cannot be caused by heat flow of the type considered above. Moreover, the magnitude of the correction to the thermodynamic slope is small; e.g., 0.0024 ppm/ $^\circ\text{K}$ at 4 $^\circ\text{K}$. Thus, it is concluded that the presence of a temperature gradient can not produce a maximum in the Young's-modulus-versus-temperature curve of niobium.

APPENDIX B: CONVERSION OF STIFFNESS CONSTANTS TO YOUNG'S MODULUS

The reciprocal of Young's modulus is given by the expression⁴³

$$1/Y = S_{11} - 2(S_{11} - S_{12} - \frac{1}{2}S_{44})\Gamma(l, m, n), \quad (\text{B1})$$

where S_{11} , S_{12} , and S_{44} are the compliance moduli referred to the cubic axes. These moduli are related to the stiffness moduli by the expressions⁴⁴

$$S_{11} = (C_{11} + C_{12}) / (C_{11} - C_{12})(C_{11} + C_{12}), \quad (\text{B2a})$$

$$S_{12} = -C_{12} / (C_{11} - C_{12})(C_{11} + 2C_{12}), \quad (\text{B2b})$$

and

$$S_{44} = 1/C_{44}. \quad (\text{B2c})$$

⁴² A. Calverley, K. Mendelssohn, and P. M. Rowell, *Cryogenics* **2**, 29 (1961).

⁴³ J. F. Nye, *Physical Properties of Crystals* (Oxford University Press, London, 1957) p. 145.

⁴⁴ J. F. Nye, *Physical Properties of Crystals* (Oxford University Press, London, 1957), p. 147.

From velocity of sound measurements along the [110] axis, certain combinations of the stiffness constants are obtained; i.e., $C_L \equiv \frac{1}{2}(C_{11} + C_{12} + 2C_{44})$ is determined from the speed of longitudinal waves, $C' \equiv \frac{1}{2}(C_{11} - C_{12})$ is determined from the speed of shear waves with particle motion in the [1 $\bar{1}$ 0] direction, and $C \equiv C_{44}$ is determined from the speed of shear waves with particle motion in the [001] direction. Substitution of Eqs. (B2) into Eq. (B1) yields

$$Y = \frac{CC'(3C_L - C' - 3C)}{C(C_L - C) + (C' - C)(3C_L - C' - 3C)\Gamma(l, m, n)}. \quad (\text{B3})$$

Young's modulus is expressed in terms of C_L , C' , and C , since these quantities are reported by Alers and Waldorf.³⁵

The moduli variations measured in this investigation and by Alers and Waldorf are less than 200 ppm. Therefore $(\Delta Y/Y)$ is expressed in differential form; viz.,

$$(\Delta Y/Y) = (1/Y)[C(\partial Y/\partial C)(\Delta C/C) \\ + C'(\partial Y/\partial C')(\Delta C'/C') + C_L(\partial Y/\partial C_L)(\Delta C_L/C_L)]. \quad (\text{B4})$$

The appropriate partial derivatives are evaluated to be

$$\partial Y/\partial C = C'^2(N^2\Gamma - C^2)/D^2, \quad (\text{B5a})$$

$$\partial Y/\partial C' = C^2[(C_L - C)(N - C') - N^2\Gamma]/D^2, \quad (\text{B5b})$$

and

$$\partial Y/\partial C_L = (CC')^2/D^2, \quad (\text{B5c})$$

where $N = (3C_L - C' - 3C)$ and $D = C(C_L - C) + (C' - C)N\Gamma$. When the values of $\Gamma(l, m, n)$ listed in Table I and C , C_L , and C' from Ref. 35 are substituted into Eqs. (B4) and (B5), Eq. (B4) reduces to

$$(\Delta Y/Y) = 0.535(\Delta C/C) \\ + 0.369(\Delta C'/C') + 0.097(\Delta C_L/C_L),$$

and

$$(\Delta Y/Y) = 0.461(\Delta C/C) \\ + 0.436(\Delta C'/C') + 0.103(\Delta C_L/C_L)$$

for the deformed MRC and BTL crystals, respectively.